Measurement of the absolute neutron efficiency for a NE-102A scintillator in the energy range 2–7 MeV using the associated particle technique

A. Varela, R. Policroniades, J. Lopez and R. Maggi
Laboratorio del Acelerador Tandem, ININ, México

Recibido el 11 de marzo de 1992; aceptado el 11 de agosto de 1992

Abstract. This paper describes the absolute neutron detection efficiency calibration of a NE-102A[1] scintillator detector in the energy range 2–7 MeV. The neutrons were obtained by means of the D(d, n) ^{3}He reaction, and the neutron beam characteristics were determined using the associated particle technique (APT). The efficiency measurements are compared with the calculations from a Monte Carlo code (SAN REMO).

Resumen. Este artículo presenta la calibración absoluta a neutrones de un detector NE-102A en el intervalo de energía 2–7 Mev. El haz de neutrones monoenergético se obtuvo usando la reacción D(d, n) ^{3}He, y las características del mismo fueron determinadas usando la técnica de la partícula asociada (APT). Las medidas de eficiencia se comparan con las obtenidas mediante el cálculo de un programa Monte Carlo (SAN REMO).

PACS: 29.25.Dz; 29.30.Hz

1. Introduction

Neutron detector efficiency determinations are necessary for cross section measurements, which are fundamental in reactor design. Moreover, a facility which provides a monoenergetic neutron beam of known flux is a useful versatile instrument for basic and applied nuclear physics. For instance, the use of this kind of facilities in proving theoretical explanation of reaction mechanisms or nuclear structure models, as well as studies of the absorbed energy and radiobiological applications, are known [1].

It is well established that the Associated Particle Technique (APT) [2] used with the D(d, n) ^{3}He reaction provides a monoenergetic neutron beam of known flux in a wide energy range. The APT uses a coincidence between the neutron and the associated helium particle, so special care must be taken in order to resolve the helium peak from the other charged particle products scattered from the target.

In order to solve this problem, it is common practice to use thin self supported deuterated polyethylene targets and a solid state "ΔE" totally depleted silicon surface barrier detector with a thickness chosen in agreement with the range of helium particles in silicon [3]. The use of "$E - \Delta E$" telescopes has been reported [4], and in a more recent work a time zero (Micro Channel Plate)-SSSB detector telescope was used [5]. By using

[1]Nuclear Enterprises LTD, England.

this technique the neutron flux is known within the uncertainty associated to the helium recording, and in practice the spatial distribution of the neutron beam (neutron cone) is determined by the kinematics of the reactions involved, in agreement with the solid angle subtended by the charged particle detector.

Using the APT and an appropriate experimental setup, it is possible to carry out efficiency measurements with the neutron detector placed so that the front face encloses the neutron cone. In this way, if $N_{^3\mathrm{He}}$ is the number of ^{3}He recorded and N_c the number of n–^{3}He coincidences, then

$$\epsilon(E_n, B) = \frac{N_c}{N_{^3\mathrm{He}}} f \tag{1}$$

is the efficiency of the neutron detector, with f a correction factor that takes into account neutron attenuation due to the scattering chamber walls, E_n is the neutron energy and B, the bias level imposed on the scintillator, which defines a threshold energy for the neutron interactions.

In this report the absolute efficiency measurements of a NE-102A (5.0 cm diameter $\times$7.62 cm thick) neutron plastic detector, and their comparison with an analytical approximation [6] and a Monte Carlo Code (SAN REMO [7]) calculation, are presented. We also present results in the proton light response of the scintillator and the method used in setting the bias level B on the scintillator (Eq. 1).

The experiment was performed using the associated particle time of flight facility [8] at the Tandem Laboratory of the Instituto Nacional de Investigaciones Nucleares (México).

2. EXPERIMENTAL DETAILS

a) Set up

Deuteron beams, with energies from 3.0 to 8.0 MeV of the 6.0 MV ININ Tandem accelerator, were collimated to 1.5 $\times$ 2.5 mm at the entrance of the scattering chamber (shown in Fig. 1) by a set of rectangular slits and directed towards thin self supported (100 to 300 μg/cm^2) deuterated polyethylene targets, made following the method described in Ref. [9]) and placed at the center of the stainless steel scattering chamber. The deuteron beam was stopped in a Faraday cup 4 m away. A turbomolecular pump connected to the scattering chamber assures good vacuum conditions ($\simeq 10^{-6}$ Torr) during the experiment. For necessary target changes, the total time spent, including atmospheric pressure admission, target substitution and scattering chamber evacuation, was typically less than 30 minutes.

Since polyethylene is a low temperature burning material, we used a rotating target assembly, described in Ref. [8]. During bombardment, the beam follows a circular path along the polyethylene film, avoiding a fast target deterioration.

The associated particle (AP) detector (totally depleted silicon surface barrier detector 30 μm thick), was chosen according to the ^{3}He range in silicon and housed in a detector support assembly 6.5 cm away from the target. This detector assembly uses two limiting

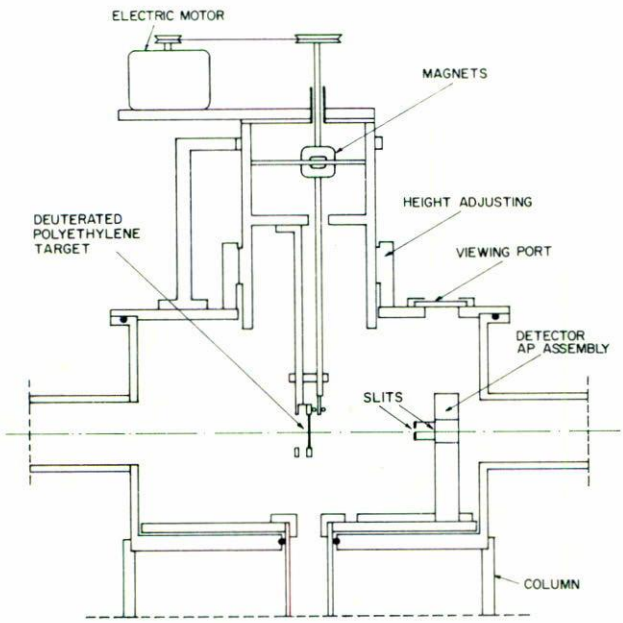

FIGURE 1. Schematic sectional view of the APT scattering chamber (not in scale).

circular slits 1.5 mm (entrance) and 2.5 mm (exit) which, according with the kinematics of the d–D reaction, provides a neutron cone enclosed by the 5.0 cm diameter front face of NE-102A neutron detector, positioned during the efficiency measurements at a distance ranging from 14 cm to 20 cm from the target. The neutron detector assembly consists of a sliding frame with 3 degrees of freedom for fixing the height, the distance and the angle of the neutron detector with respect to the usual target-beam direction convention, respectively.

To assure reproducibility in the neutron detector positioning, it was necessary to make use of an optical alignment reference system for taking the neutron profile data and the efficiency measurements.

The neutron beam emerges through a 130 degrees wide, 9.5 cm high and 0.8 mm thick stainless steel window. The use of this thin window minimizes the attenuation and energy spread of the neutron beam.

Typical beam intensities were 25–50 nA upon the target, giving neutron fluxes of 15 to 30 neutrons/s, in agreement with the target's thickness and the neutron detector distances used.

b) Electronics

A block diagram of the electronic arrangement used is depicted in Fig. 2. Timing signals were obtained from the photomultiplier's anode, and alternatively, from a constant fraction discriminator in the case of the AP detector. These two fast signals were sent to the "start" and "stop" inputs of a time to amplitude converter (TAC). A single channel analyzer window was defined to select the proper fast coincidence (TOF) events and, sub-

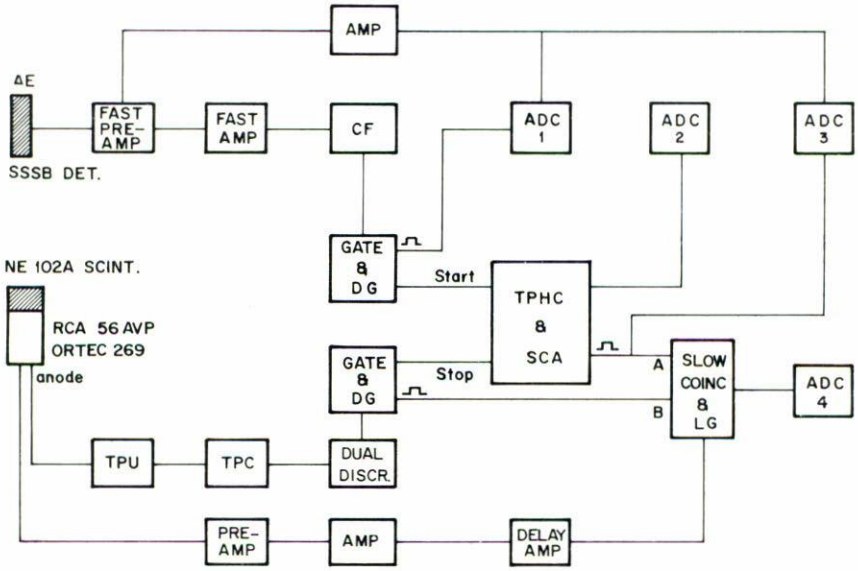

FIGURE 2. Block diagram of the electronic arrangement used in the APT neutron spectroscopy. Legend: FAST PRE-AMP = preamplifier, Ortec 142B; Fast AMP = fast timing amp., Ortec 484; AMP. = Amplifier, Ortec 485; CF = constant fraction Disc., Ortec 474A; GATE & D.G. = gate and delay generator, Ortec 416A; TPU = time pickoff unit, Ortec 260; TPC = time pickoff control, Ortec 403A; DUAL DISCR. = dual discriminator, EG&G TR104S/N; TPHC & SCA = time to pulse hight converter/SCA, Ortec 467; DELAY AMP. = delay amplifier, Ortec 427; ADC = analog to digital converter, Canberra 8075.

sequently, this signal was then used to gate concurrent linear signals from the scintillator and the AP detector.

Finally, the linear signal from the TAC and the gated and non gated linear signals from each detector, were simultaneously recorded in a Canberra-Series 88 multichannel analyzer (Conn., USA). Figures 3 and 4 show typical charged particle and time of flight (TOF) spectra, respectively.

3. MEASUREMENTS

a) Neutron beam profile

Since a neutron cross section measurement programme is the final goal of our facility, the overall performance and reproducibility was an important point during the efficiency measurements. We initiated the calibration of the neutron detector with the experimental evaluation of the neutron beam profile, which is a function of the beam spot, the aperture of the AP detector slits and, in the case of the horizontal plane, of the kinematics of the reaction. The knowledge of these parameters defines the spatial distribution of the neutron beam (neutron cone) which is important to know for a neutron cross section measurement, and in the case of the efficiency measurements, for the positioning of the neutron detector and the evaluation of the intercepted area on the detector front face by the neutron beam.

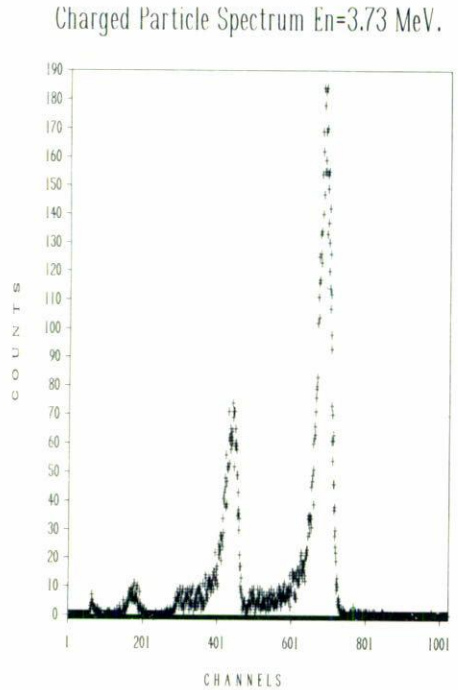

FIGURE 3. Typical (gated) charged particle spectrum corresponding to deuteron beam energy $E_d = 4.0$ MeV, $E(^3\text{He}) = 3.54$ MeV; also shown are ^{4}He groups coming out from $^{12}\text{C}(\text{d},\alpha)\,^{10}\text{B}$ reaction. High energy peak corresponds to ^{3}He.

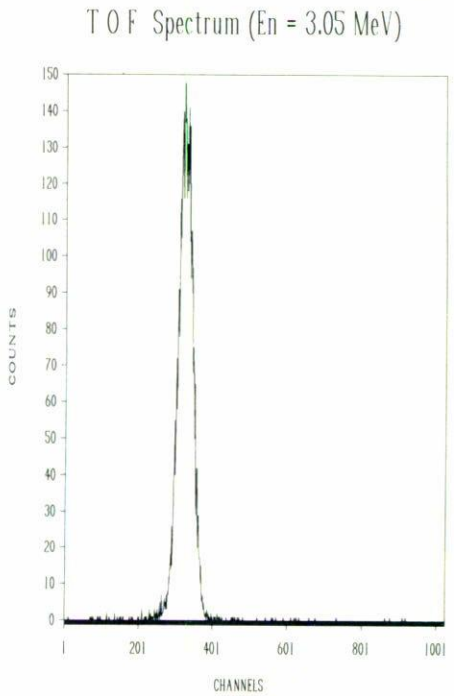

FIGURE 4. Time of flight spectrum (typical) for $E_n = 3.05$ MeV, FWHM = 2.8 ns (1 ns = 16.4 channels).

Figure 5 shows a typical neutron beam profile obtained for a neutron energy $E_n = 3.73$ MeV. This profile was measured with the neutron detector positioned 17.3 cm away from the target, and moved horizontally in steps of one degree. The vertical scale gives a relative measure of the ratio $N_c/^3$He counts. The solid line is a calculated profile assuming the geometry shown in Fig. 6 [6]: the intersection of an ellipse (neutron cone cross section) and a circle (neutron detector's front face). The differences between the measured and the calculated beam profiles are mainly due to edge effects.

b) Efficiency measurements

The detector calibration was done for various selected neutron energies using the electronic arrangement shown in Fig. 2. As stated, the neutron detector was positioned so that the detector front face encompassed the neutron beam. With this assumption, the detector efficiency is given by Eq. (1).

The experimental results for the efficiency measurements are summarized in Fig. 7; these measurements were taken within 1–1.2% counting statistical uncertainty. The solid curve corresponds to the analytical calculation [6] taking into account single and double H and C scattering, and the dashed line to the Monte Carlo ("San Remo" code [7]) calcu-

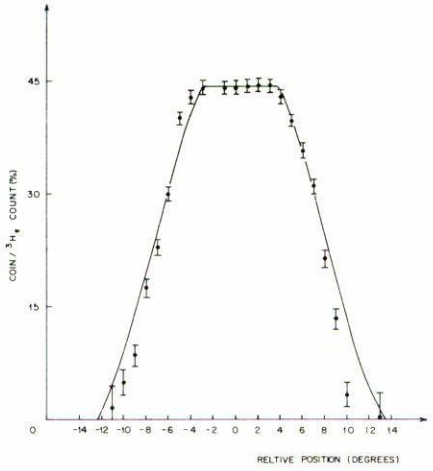

FIGURE 5. Horizontal beam profile measurement (%) and calculations (solid line) for neutron energy $E_n = 3.73$ MeV.

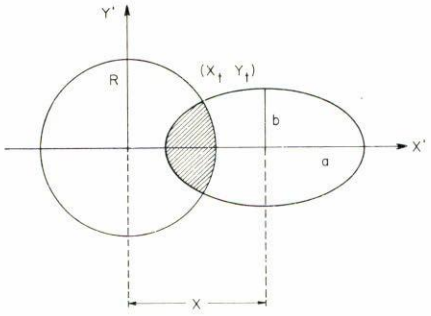

FIGURE 6. Geometrical parameters involved in the neutron beam profile's calculation, asuming the intersection of a circle (detector's front face) and an ellipse (neutron cone's cross section).

lation with a correcting factor $f = 0.92$, used to fit the experimental points (represented by small circles), and 50 keV equivalent electron energy bias.

c) Proton light response

The light response of the recoil protons produced in the scintillator by the incident neutrons, is usually related to electron light response, owing to the fact that the total light emitted by electrons is a linear function for electron energies above 100 KeV [10].

It is a common practice in order to find a relationship between the proton and the electron light responses, to measure the scintillator's electron light response using the Compton spectra of a set of gamma sources, determining the channels corresponding to the maximums or the half-maximums of the Compton edge of each distribution, and finally, associating these channels, whichever, with the maximum Compton recoil energies

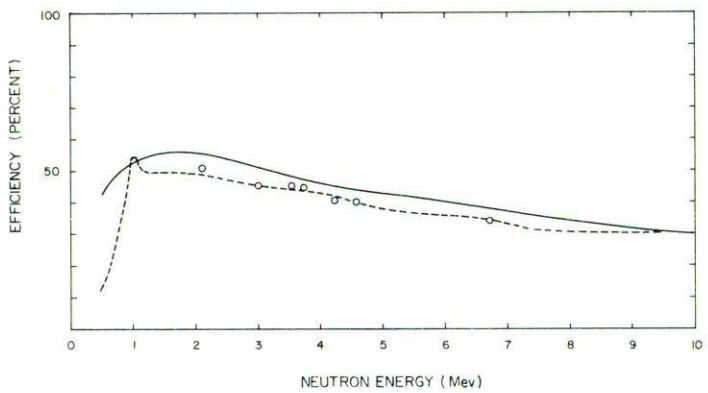

FIGURE 7. Experimental results (o) and calculated efficiency determinations, with a bias level of 50 KeV, equivalent electron energy, on the NE-102A detector. The dashed curve corresponds to the corrected Monte Carlo calculations [7], and the solid line is the fit related to the analytical approximation.

given by

$$E_c = \frac{2E\gamma^2}{2E\gamma + 0.511} \quad \text{(MeV)}.$$

However, in both cases, an energy shift will occur because the points do not precisely correspond to these characteristic energies. Moreover, it is a well established fact, that the E_c's positions are function of the detector's dimension, its energy resolution and the gamma energy [11], and should be placed somewhere in between the maximum and the half-maximum of the Compton edge distribution.

To avoid this disadvantage, we performed [12] an adequate measurement of the scintillator's electron response using a fast-slow coincidence arrangement which selects the maximum Compton recoil events.

Figure 8 depicts a block diagram of the electronic arrangement used for this purpose. The system uses a coincidence between the maximum Compton recoil and 180° backscattered photon. Figure 9 shows some typical spectra, and Table I contains the relevant results in maximum recoil energy units. By using this scintillator's electron response it is simple to verify, during the experiment development, the bias level by taking Compton distributions of a pair of gamma sources.

For comparison, we recorded the proton recoil spectra produced during the efficiency measurements, assigning the point half down the maximum energy edge of this distribution as the neutron energy. Figure 10 shows a typical proton recoil spectrum obtained, and Fig. 11 summarizes the measured proton versus electron equivalent energy response curve. For this energy interval, our results agree quite well with those presented in 1969 by Craun and Smith [14] and reviewed by Fowler *et al.* [6] in 1980.

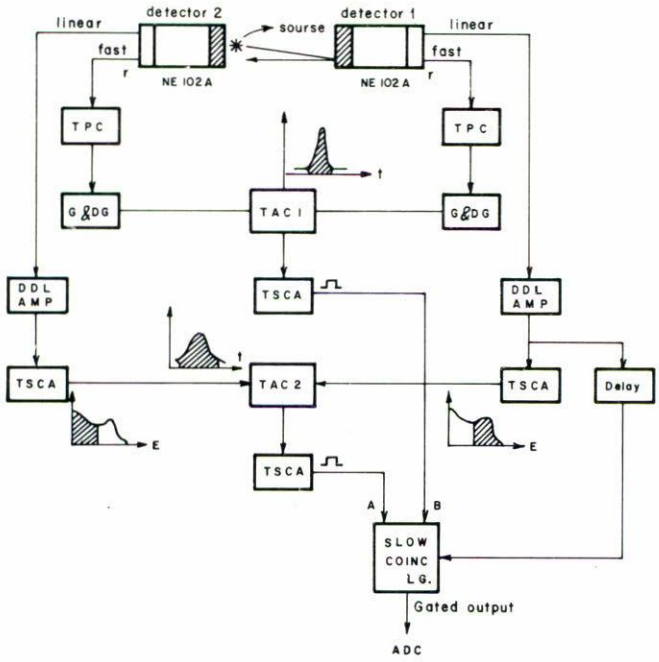

FIGURE 8. A block diagram of the electronic arrangement used to obtain the gamma response of the NE-102A scintillator.

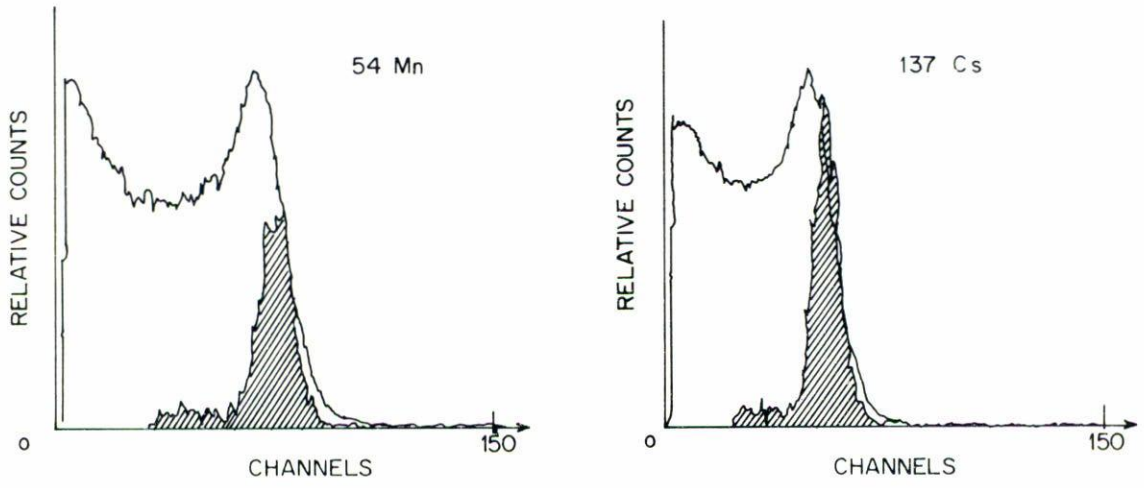

FIGURE 9. Typical gamma Compton spectra for ^{137}Cs and ^{54}Mn, superimposed with their maximum Compton recoil energy distributions (shown in shadowed areas).

TABLE I. Experimental results in maximum recoil energy units, concerning the gamma calibration of our NE-102A scintillator detector.

Source	Energies (MeV)				$\frac{E_c - E_{max}}{E_c}$	$\frac{E_{1/2} - E_c}{E_c}$
	γ	Compton	Maximum	Half Compton		
^{22}Na	0.511	0.341	0.319	0.388	6.5	13.8
^{137}Cs	0.662	0.478	0.443	0.516	7.3	7.9
^{54}Mn	0.840	0.644	0.592	0.681	8.1	5.8
^{22}Na	1.275	1.062	1.014	1.141	4.5	7.4
					$6.6 \pm 1.5\%$	$8.7 \pm 3.5\%$

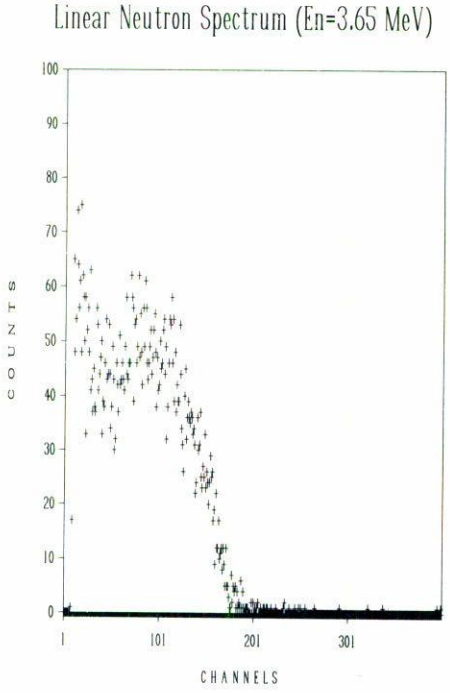

FIGURE 10. Typical linear neutron spectrum, $E_n = 3.65$ MeV.

4. CALCULATIONS

a) Analytical calculations

The scintillator's efficiency considering single n–H and n–C scattering is given by

$$\epsilon(E_n, B) = \frac{\Sigma_H(E_n)}{\Sigma_T(E_n)} \left(1 - \frac{B}{E_n}\right) \left(1 - e^{t\Sigma_T(E_n)}\right)$$

where $\Sigma_H = n_H \sigma_H$ is the hydrogen macroscopic cross section for the neutron energy E_n,

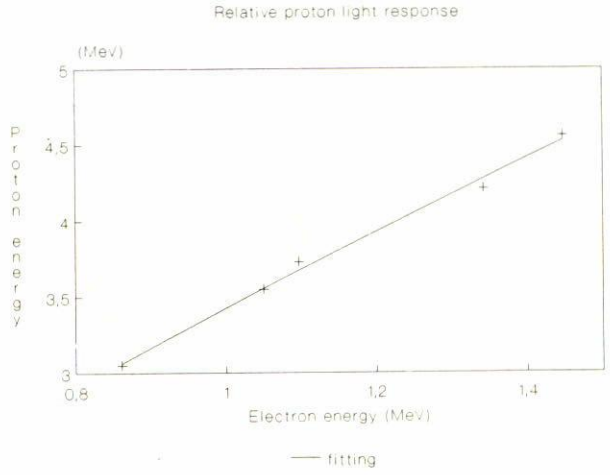

FIGURE 11. Experimental equivalent energy electron versus proton light response curve (+), together with a (parabola) fit for the energy interval shown.

and $\Sigma_T = (\Sigma_H + \Sigma_C)$ —with $\Sigma_C = n_C\sigma_C$—, is the corresponding total macroscopic cross section for this energy, B is the bias level, and t the detector's thickness.

However, in order to have a more representative picture, a formalism that takes into account single and multiple scattering, originally described by Drosg [13] and Fowler [6] and used previously by us [2], was employed.

b) Monte Carlo calculations

A more convenient calculation for the neutron detector efficiency calibration is to use a Monte Carlo code calculation, modified by a correcting factor, to fit the experimental data in order to extend the useful neutron energy interval. For this purpose we used the "SAN REMO" Monte Carlo code [6], which was reported previously by some of us in ref.(2), with the proper parameters for NE-102A scintillator and the use of a CYBER computer (CDC Corp., USA). As stated previously, Fig. 7 summarizes these and other results pertinent to the efficiency calibration.

5. CONCLUSIONS

As one task in our work was to check the suitability of the neutron time of flight facility, we found that this calibration procedure is quite adequate for our neutron cross section measurement programme, and it is now currently used at the Tandem Laboratory in total and differential cross section measurements for neutron energies ranging from 2 to 10 MeV for elements like Cr, V, and Ti.

The overall performances of the NE-102A scintillator turned out better, due to its higher efficiency, compared with the liquid scintillator NE-213 used previously by us in Ref. [8]. The procedure or method followed by us to measure and check the bias level of organic scintillators, is a very useful tool for neutron spectroscopy experiments.

ACKNOWLEDGEMENTS

We are very grateful to Prof. J. Calvillo for useful discussions and reading the manuscript. We are also indebted to the Tandem operator staff for technical assistance during the experiment.

REFERENCES

1. S. Cierjacks, *Neutron Sources for Basic Physics and Applications*, p. 1; S. Cierjacks, Ed., Pergamon press (1983), and references therein; J. Csikai, *Fast Neutron Generators*, 2 vols., CRC Publ. Co. (1987), New York, USA, and references therein.
2. R. Cherubini, G. Moschini, R. Nino, R. Policroniades and A. Varela, *Nuclear Instruments and Methods* **A269** (1988) 623.
3. D.G. Schuster, *Nuclear instruments and Methods* **76** (1969) 353.
4. C.M. Bartle *et al., Nucl. Inst. & Meth.* **144** (1977) 437.
5. C. Cernigoi, G.V. Margagliotti, C. Tuniz, R. Cherbini, A. Varela and G. Moschini, *Nucl. Instr. & Meth.* **A270** (1988) 232.
6. J.L. Fowler, *et al., Nucl. Instr. & Meth.* **175** (1980) 4497) M.
7. Anghinolfi *et al., Nucl. Inst. & Meth.* **165** (1979) 2178 8.
8. G. Aguirre, B. Sc. Thesis, Fac. of Sciences, UNAM (1978) Mexico, unpublished.
9. C.M. Bartle and H.O. Meyer, *Nucl. Instr. & Meth.* **112** (1973) 61; M. Bruno *et al., Lett. Nuovo Cim.* **2** (1978) 556.
10. K.F. Flynn, *Nuclear Instruments and Methods* **27** (1964) 13.
11. G. Dietze and H. Klein, *Nucl. Instr. & Meth.* **193** (1982) 549; G.Dietze, *IEEE Trans. Nucl. Sci.* **NS-26** No. 1 (1979) 398.
12. R. Cherubini, G. Moschini, R. Nino, R. Policroniades and A. Varela, *Nuclear Instruments and Methods* **A281** (1989) 349.
13. M. Drosg, *Nuclear Instruments and Methods* **105** (1972) 573.
14. R. Craun and D. Smith, *Nucl. Inst. & Meth.* **80** (1969) 239.